Figure S1. *Related to Figure 2 and Figure 3*

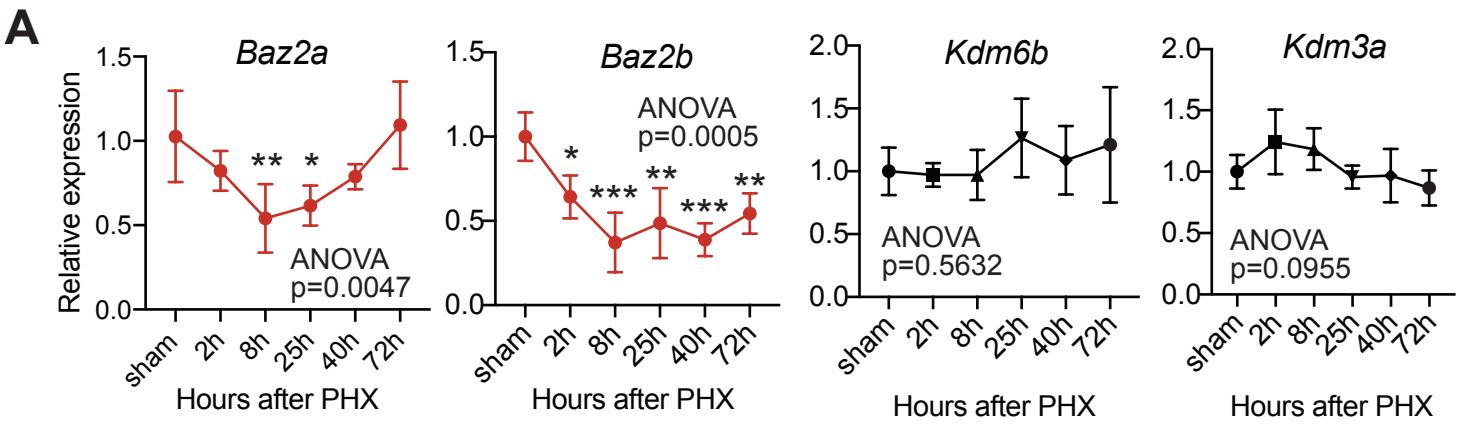

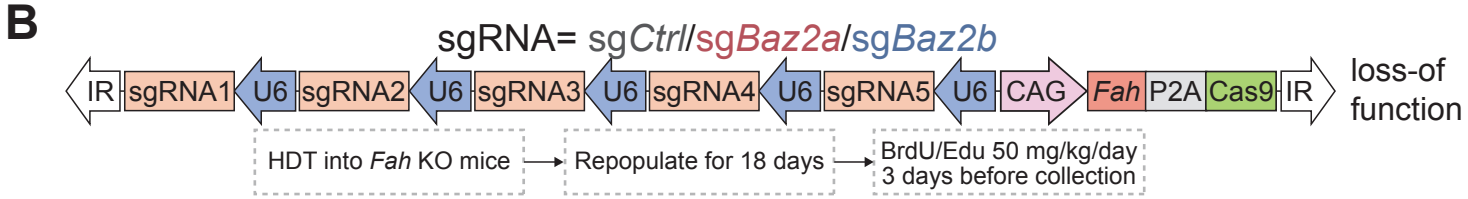

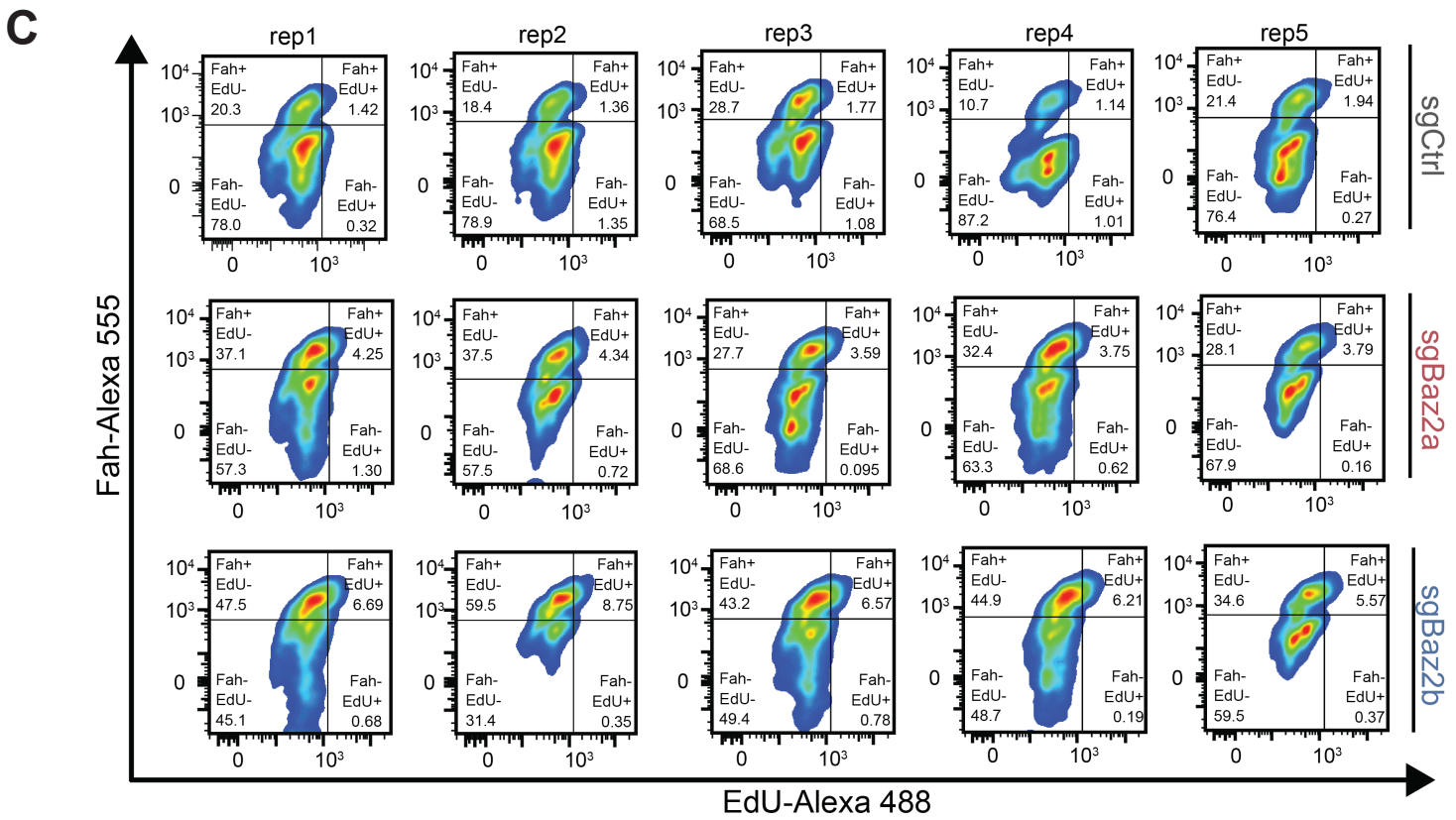

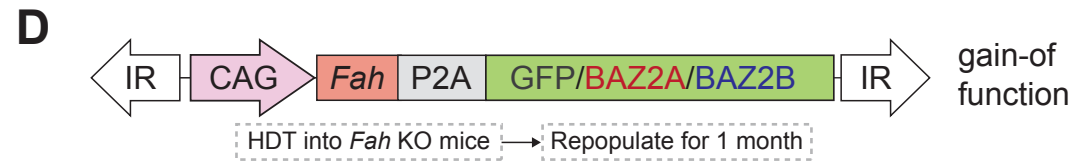

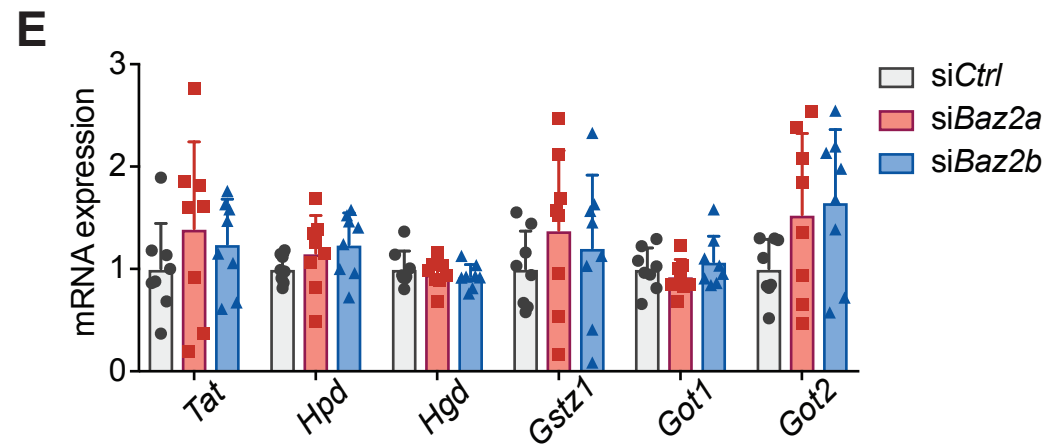

Supplemental Figure S1. Validation of *Baz2a* and *Baz2b* as suppressors of liver regeneration. Related to Figures 2 and 3.

A. Real-time qPCR analysis on *Baz2a*, *Baz2b*, *Kdm6b*, and *Kdm3a* mRNA expression at multiple time points after 70% PHx (sham surgery: n = 3 mice; 2h: n = 4 mice; 8h: n = 5 mice; 25h: n = 3 mice; 40h: n = 4 mice; 72h: n = 3 mice).

B. Schema for loss-of-function validation experiments for *Baz2a* or *Baz2b* using *Fah* KO mice. The Sleeping Beauty transposon expresses *Fah*, *Cas9*, and five distinct sgRNAs targeting either *Baz2a* or *Baz2b*. 18 days after HDT, liver tissues were collected for immunofluorescence (IF) and flow cytometry analysis. A dose of BrdU or EdU (50 mg/kg) was given to mice every day starting 3 days before tissue collection.

C. Flow cytometry analysis of individual livers treated with sgRNAs targeting *Baz2a* or *Baz2b*. 18 days after receiving non-targeting sgRNAs or sgRNAs targeting either *Baz2a* or *Baz2b,* hepatocytes were perfused and analyzed. EdU was given IP at 50 mg/kg per day starting 3 days before tissue collection. Hepatocytes were stained with an Alexa 555 conjugated antibody for mouse FAH. EdU was stained with Alexa 488. The number of FAH+ hepatocytes reflects the amount of repopulation that occurred during the 18-day period. The percentage of FAH+; EdU+ cells reflects the fraction of rescued cells undergoing DNA synthesis during the 3-day period prior to collection (n = 5, 5, 5 mice).

D. Schema of gain-of-function experiments for human *BAZ2A* and *BAZ2B* using *Fah* KO mice. The Sleeping Beauty transposon used for gain-of-function validation expresses *Fah* and either human *BAZ2A* or *BAZ2B*. Liver tissues were collected for IF analysis one month after HDT.

E. Expression of tyrosine metabolism related mRNAs as measured by qPCR in uninjured liver tissues collected in **Figure 3** (n = 8, 8, 8 mice).

All data is represented as mean ± SD. * $p<0.05$, ** $p<0.01$, *** $p<0.001$, **** $p<0.0001$. In (**A**) and (**E**), significance was assessed by One-Way ANOVA followed by Dunnett's multiple comparisons testing.

Figure S2. *Related to Figure 4*

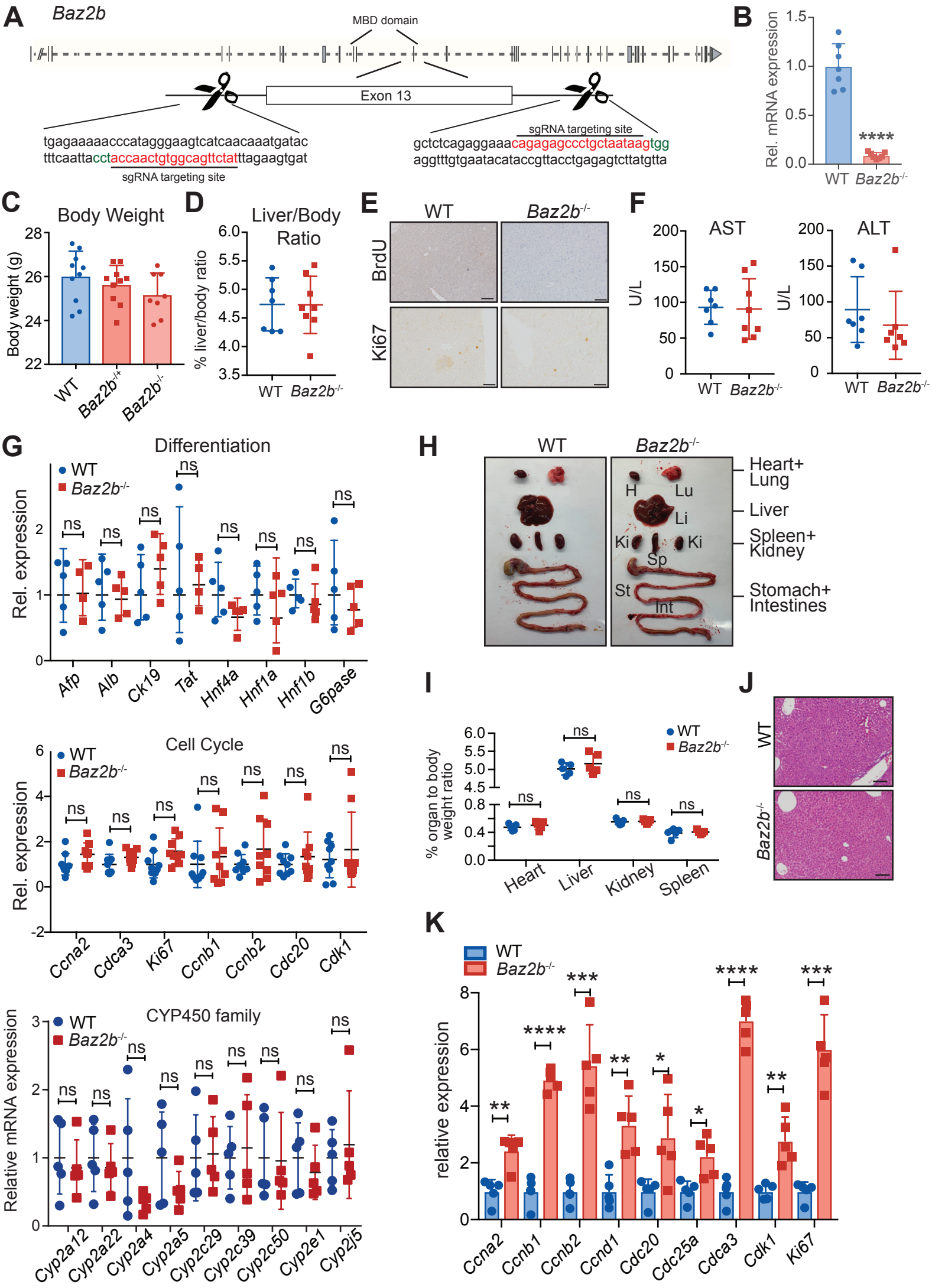

Supplemental Figure S2. *Baz2b* knockout mice have preserved liver function and improved liver regeneration after injury. Related to Figure 4.

A. Diagram showing the design of *Baz2b*$^{-/-}$ mice generated by CRISPR deletion using synthetic sgRNAs. Protospacer-adjacent motif (PAM) sequences are highlighted in green.
B. qPCR showing the reduction of *Baz2b* mRNA in KO liver tissues (n = 7, 7 mice).
C. Body weights of 8-10 week old whole body *Baz2b* WT, heterozygous, and KO mice (n = 10, 10, 8 mice).
D. Liver to body weight ratios of 8-week-old WT and *Baz2b*$^{-/-}$ mice (n = 7, 8 mice).
E. Representative BrdU and Ki67 IHC on uninjured WT and *Baz2b* KO mice (BrdU: scale bar = 100 μm; Ki67: scale bar = 50 μm).
F. Serum AST/ALT levels of 8-week-old WT and *Baz2b*$^{-/-}$ mice (AST: n = 7, 8 mice; ALT: n = 7, 7 mice).
G. qPCR analysis of differentiation, cell cycle, and CYP450 family related gene expression in livers from 8-week-old WT vs. KO livers (differentiation: n = 5, 5; cell cycle: n = 9, 9; CYP450 family: n = 5, 5 mice).
H. Representative gross morphology of multiple organs from 1.5-year-old WT and *Baz2b*$^{-/-}$ mice (images are representative of n = 5, 5 male and n = 7, 5 female mice).
I. Percent organ to body weight ratios of heart, liver, kidney, and spleen in 1.5-year-old WT and *Baz2b*$^{-/-}$ mice (n = 5, 5 mice).
J. Representative H&E images of livers from 1.5-year-old WT and *Baz2b*$^{-/-}$ mice (scale bar = 100 μm).
K. Cell cycle gene expression in livers of 8-week-old WT and *Baz2b*$^{-/-}$ 48 hours after 70% PHx as measured by qPCR (n = 5, 5 mice).

For all panels, each point is an individual biological replicate from one mouse and data is represented as mean ± SD. * $p<0.05$, ** $p<0.01$, *** $p<0.001$, **** $p<0.0001$. For (**B**), (**D**), and (**F**), significance was assessed by Student's t-test. For (**C**), significance was assessed by One-Way ANOVA followed by Tukey's multiple comparisons test. For (**G**), (**I**), and (**K**), significance was assessed by multiple t-tests corrected with the Holm-Sidak method.

Figure S3. *Related to Figure 5*

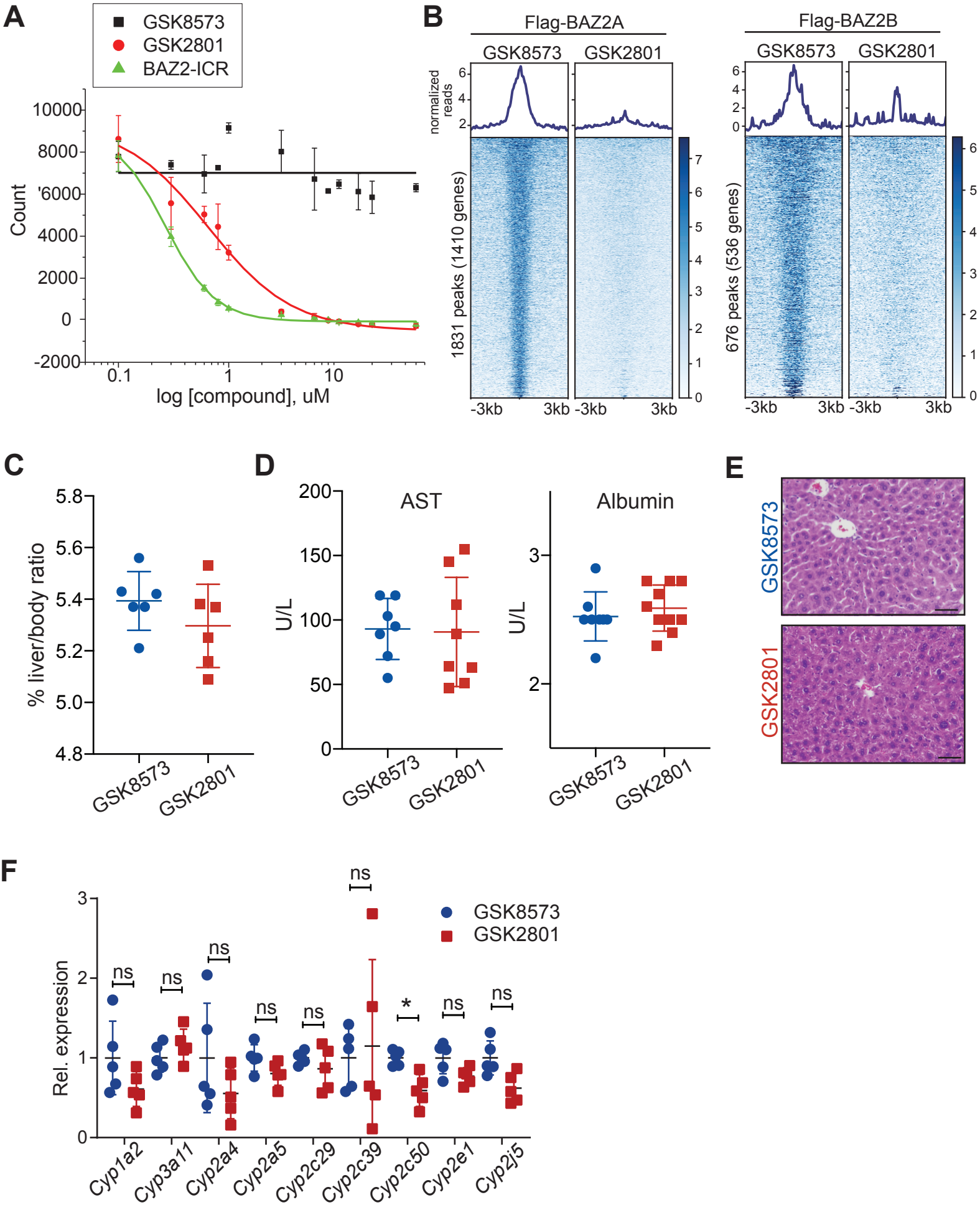

Supplemental Figure S3. Chemical BAZ2 inhibition disrupted the binding of BAZ2A and BAZ2B to chromatin and did not have an effect on normal liver function. Related to Figure 5.

A. An AlphaScreen experiment showing the affinities of GSK2801 and BAZ2-ICR to the BAZ2B bromodomain.
B. ChIP-seq of Flag-BAZ2A and Flag-BAZ2B in mouse liver H2.35 cells treated with GSK8573 (control drug) or GSK2801 (BAZ2 inhibitor). GSK2801 disrupts the binding of either BAZ2A or BAZ2B to chromatin. The plot encompasses 3 kb around peak centers.
C. In **C-F**, mice were given either GSK8573 or GSK2801 (30 mg/kg IP daily) for a total of 5 days, after which liver tissues or serum were collected. In **C**, liver to body weight ratios are shown (n = 6, 6 mice).
D. Serum AST (n = 7, 7 mice) and albumin (n = 8, 10 mice) levels.
E. Representative H&E images of liver tissues (scale bar = 50 μm).
F. qPCR analysis of CYP450 gene expression in uninjured livers of mice given either GSK8573 or GSK2801 for a total of 5 days (n = 5, 5 mice).

For all panels, each dot is an individual biological replicate from one mouse and data is represented as mean ± SD. * $p<0.05$, ** $p<0.01$, *** $p<0.001$, **** $p<0.0001$. For (**C**) and (**D**), significance was assessed by Student's t-test. For (**F**), significance was assessed by multiple t-tests corrected with the Holm-Sidak method.

Figure S4. *Related to Figure 5*

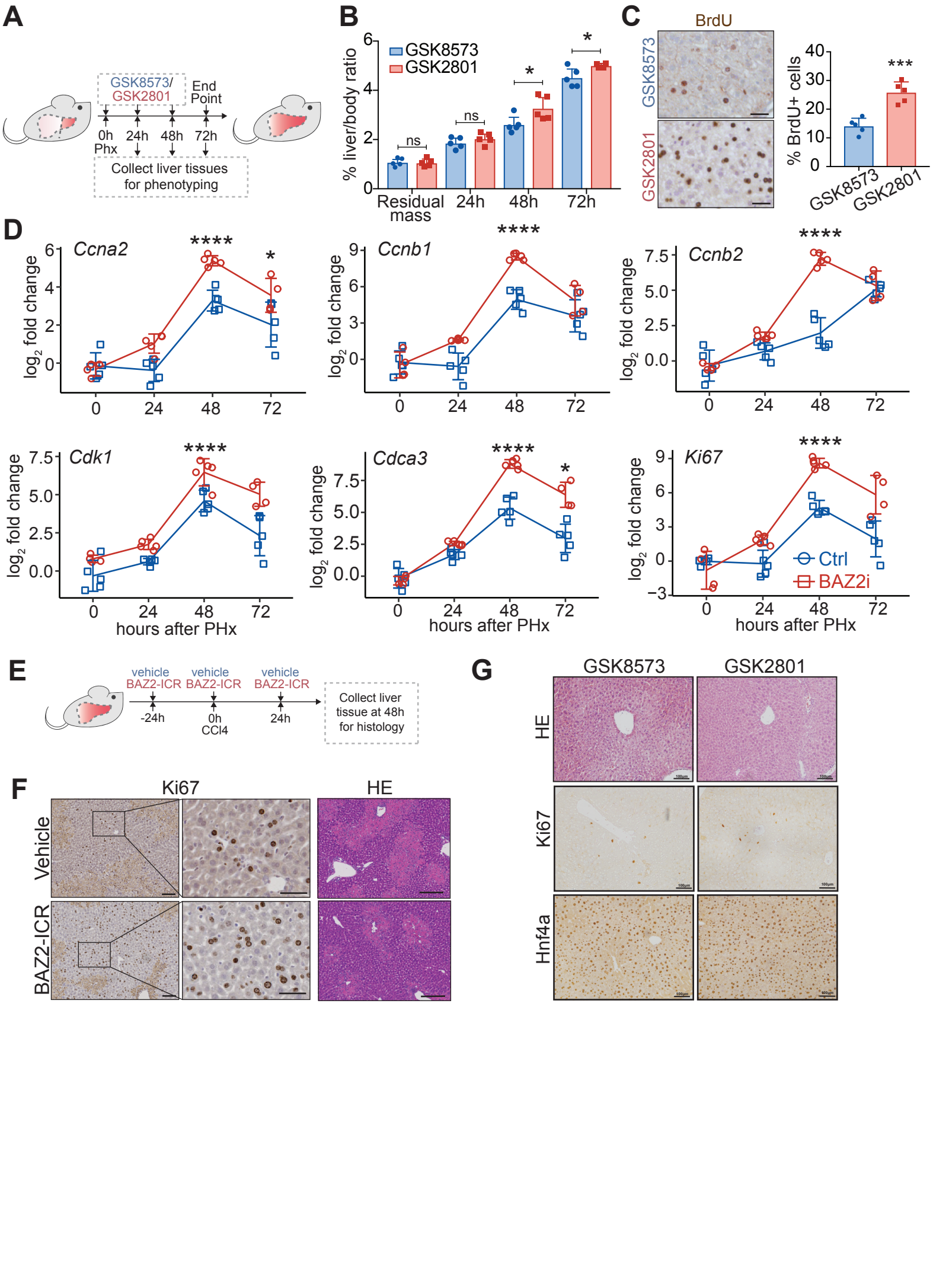

Supplemental Figure S4. Chemical inhibition of BAZ2 resulted in improved liver regeneration without compromising liver function. Related to Figure 5.

A. Schema of a time course experiment to test the effects of BAZ2 inhibition initiated at the time of liver resection. The first inhibitor doses were given IP immediately after PHx and abdominal closure. Livers were harvested 24, 48, and 72 hours after PHx.
B. Liver to body weight ratios of mice at 0, 24, 48, and 72 hours after 70% PHx (n = 5, 5 mice).
C. IHC images and quantification of BrdU+ hepatocytes 48 hours after surgery (scale bar = 50 μm; n = 5, 5 mice).
D. Cell cycle mRNA expression at multiple time points as measured by qPCR ($n \geq 5$, 4 mice for all time points).
E. Schema for the experiment in **F**. Mice were given either a vehicle control or a second BAZ2 inhibitor called BAZ2-ICR at 30 mg/kg per day starting 24 hours before an acute dose of CCl_4. Mice were euthanized and liver tissues were collected 48 hours after CCl_4 injection.
F. Representative IHC for Ki67 and HE (scale bar = 100 μm).
G. Representative H&E and IHC for Ki67 and HNF4α 8 days after APAP collected from the mice in **Figure 5L** (scale bar = 100 μm).

For all panels, each point is an individual biological replicate from one mouse and data is represented as mean ± SD. * $p<0.05$, ** $p<0.01$, *** $p<0.001$, **** $p<0.0001$. For (**B**) and (**C**), significance was assessed by Student's t-test. For (**D**), significance was assessed by Two-Way ANOVA followed by Sidak's multiple comparison testing.

Figure S5. *Related to Figure 5*

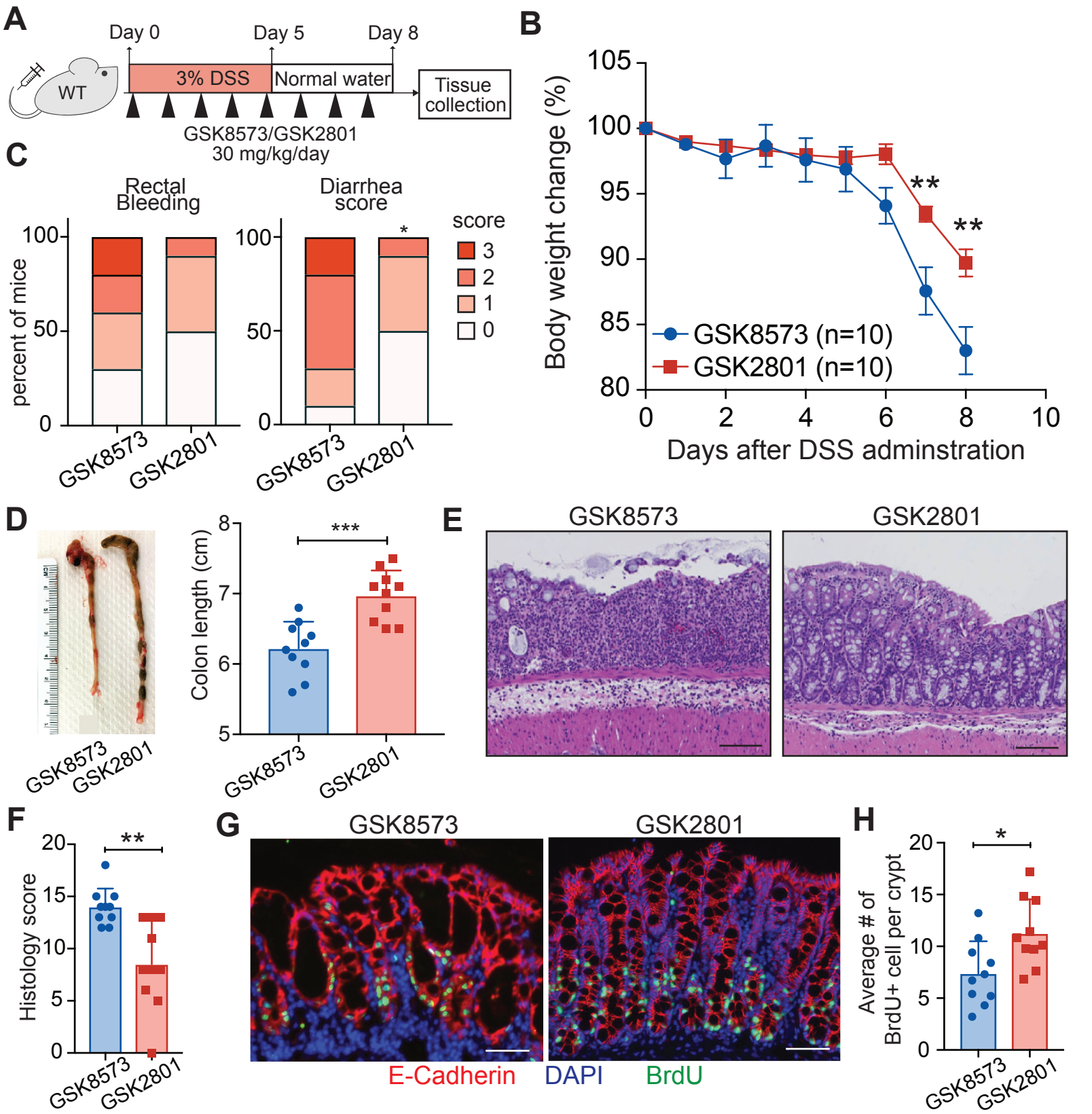

Figure S5. BAZ2 inhibition protected mice from DSS induced colitis and promoted intestinal healing. Related to Figure 5.

A. Mice were treated with GSK8573 or GSK2801 while being given 3% DSS water for 5 days, followed by regular drinking water for 3 days. This experiment was performed twice with similar results.
B. Body weight as a percentage of baseline weight (n = 10, 10 mice).
C. Rectal bleeding and stool consistency scores (see methods) were recorded 8 days after the start of DSS (n = 10, 10 mice).
D. Representative colon length on day 8, quantified on the right (n = 10, 10 mice).
E. Representative H&E images of colonic tissues in the control and BAZ2 inhibitor groups (scale bar = 50 μm).
F. Histopathology scoring (n = 10, 10 mice). See methods for the scoring criteria.
G. Composite immunofluorescence of BrdU (green), E-cadherin (red), and DAPI (blue) in the distal colon (scale bar = 50 μm).
H. Quantification of the average number of BrdU+ cells per crypt; 50 crypts were analyzed per mouse (n = 10, 10 mice).

For all data in this figure, each point is an individual biological replicate from one mouse. * $p<0.05$, ** $p<0.01$, *** $p<0.001$, **** $p<0.0001$. In (**D**), (**F**), and (**H**), data is represented as mean ± SD. Significance was assessed by Student's t-test. In (**B**), data is represented by mean ± SEM. Significance was assessed by Two-Way ANOVA followed by Sidak's multiple comparison testing. In (**C**), significance was assessed by the Chi-square test.

Figure S6. *Related to Figure 6*

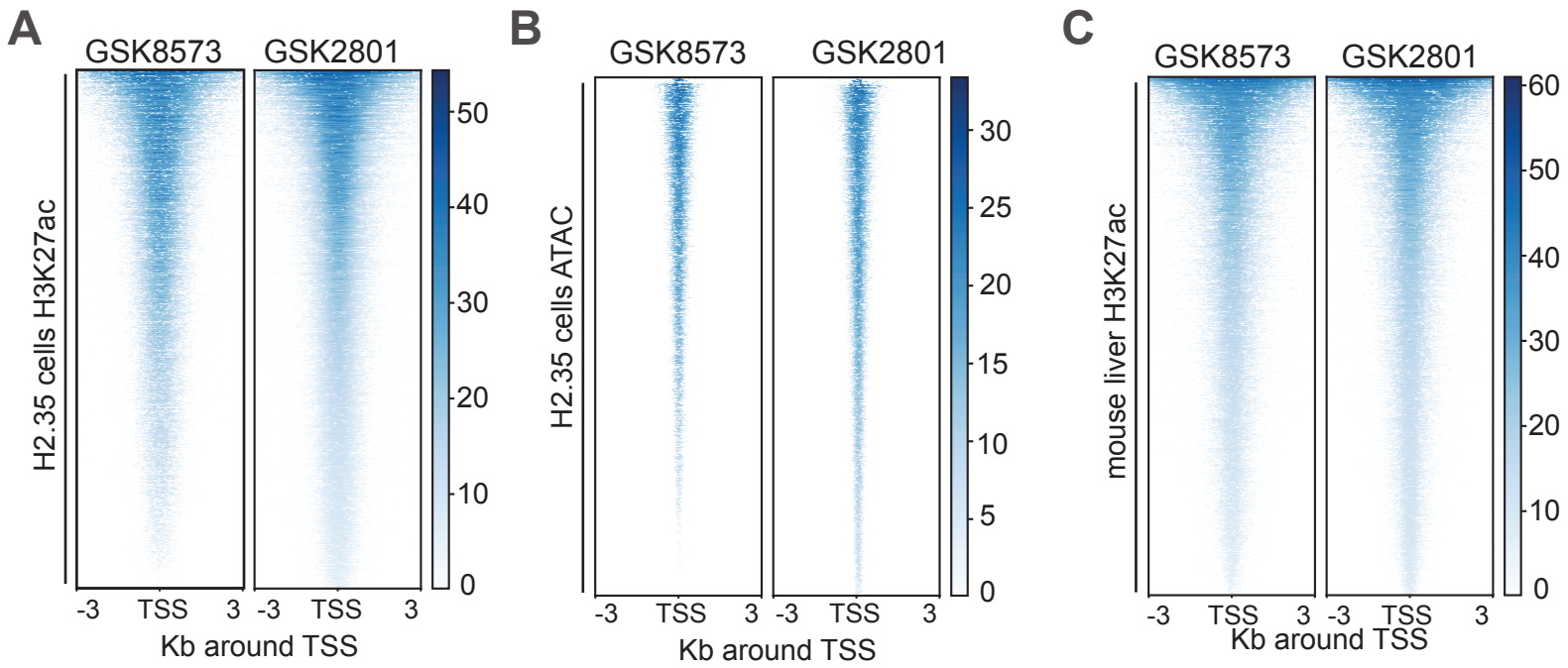

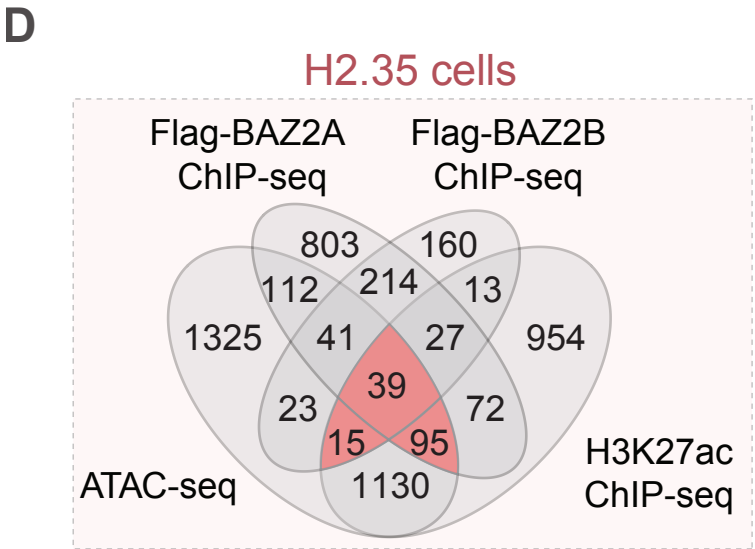

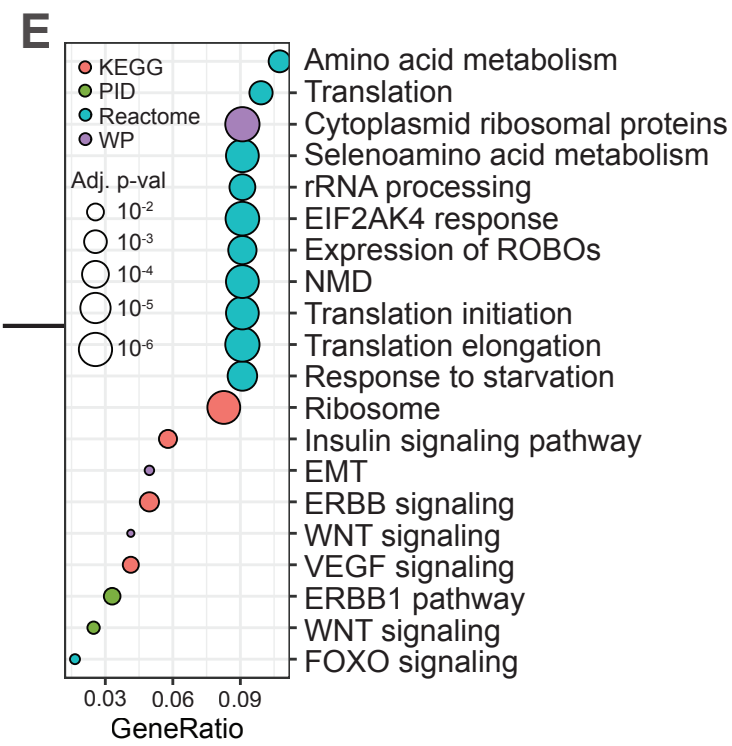

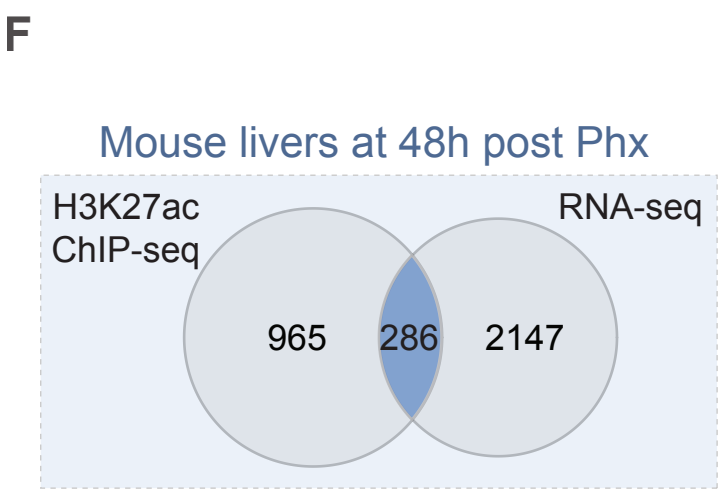

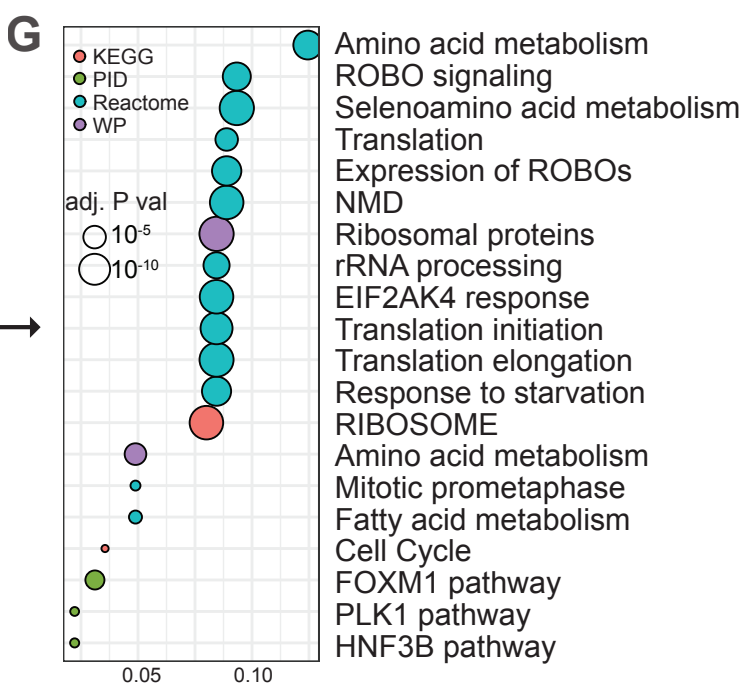

Supplemental Figure S6. BAZ2 inhibition did not alter global chromatin states but increased chromatin accessibility around ribosomal protein loci. Related to Figure 6.

A. In **A-C**, plots are combined results from three biological replicates, and the read counts were normalized based on the trimmed mean of M-values (TMM) normalization method. A 3 kb window flanking all peaks is shown. In **A**, ChIP-seq density heatmaps for H3K27ac in H2.35 cells treated with GSK8573 or GSK2801.

B. ATAC-seq density heatmaps in H2.35 cells treated with GSK8573 or GSK2801.

C. ChIP-seq density heatmaps of H3K27ac in regenerating livers treated with GSK8573 or GSK2801. The regenerating livers were obtained from the experiment in **Figure 5A.**

D. Venn diagram showing overlapping genes within differentially regulated gene sets from sequencing experiments on H2.35 cells. For ATAC-seq, differentially regulated genes were identified with a FDR < 0.05 and an absolute value of log2 fold change > 0.5. For H3K27ac ChIP-seq, differentially regulated genes were identified with a FDR < 0.05 and an absolute value of log2 fold change > 1.

E. Enriched pathways from overlapping genes identified in **Figure S6D**. The x-axis indicates the Gene Ratio, which is the percentage of the total number of differentially regulated genes in a given gene set. Circle size correlates with the adjusted p-value in the given pathway. Genes included in each pathway are listed in **Supplemental Table S3**.

F. Venn diagram showing overlapping genes within differentially regulated gene sets from sequencing experiments on 48h post-PHx mouse livers. For RNA-seq, differentially expressed genes were identified with a p-value < 0.05. For H3K27ac ChIP-seq, differentially regulated genes were identified with a FDR < 0.05 and an absolute value of log2 fold change > 1.

G. Enriched pathways from overlapping genes identified in **Figure S6F**. The x-axis indicates the Gene Ratio, which is the percentage of the total number of differentially regulated genes in a given gene set. Circle size correlates with the adjusted p-value in the given pathway. Genes included in each pathway are listed in **Supplemental Table S3**.

Figure S7. *Related to Figure 7*

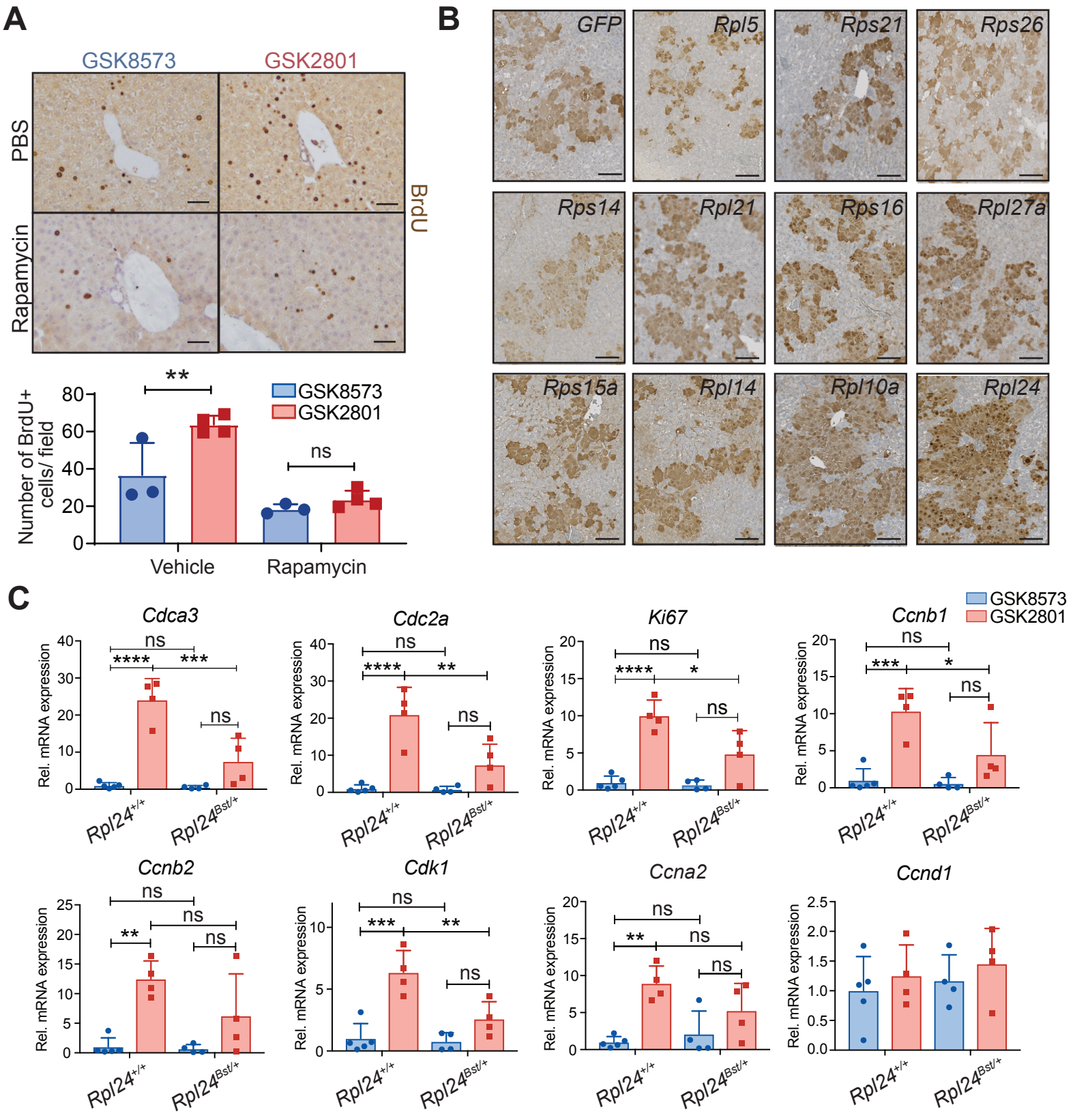

Supplemental Figure S7. Limiting increases in protein synthesis rates did not affect physiological regeneration, but suppressed augmented regeneration associated with BAZ2 inhibition. Related to Figure 7.

A. Representative IHC and quantification of BrdU on 48h post-PHx livers treated with GSK8573 or GSK2801, with or without rapamycin (scale bar = 50 μm).
B. Representative IHC images of FAH in livers overexpressing individual ribosomal proteins (scale bar = 100 μm). Experimental schema is shown in **Figure 7D**.
C. mRNA expression of cell cycle related genes in *Rpl24*$^{+/+}$ and *Rpl24*$^{Bst/+}$ livers receiving GSK8573 or GSK2801, 40 hours after PHx (*Rpl24*$^{+/+}$: n = 5, 4 mice; *Rpl24*$^{Bst/+}$: n = 4, 4 mice).

For all data in this figure, * p<0.05, ** p<0.01, *** p<0.001, **** p<0.0001. Each point is an individual biological replicate from one mouse and data is represented as mean ± SD. For (**A**) and (**C**), significance was assessed by Two-Way ANOVA followed by Tukey's multiple comparisons testing.